American Mineralogist, Volume 90, pages 672–678, 2005

Direct formation of the γ-$CaSO_4$ phase in dehydration process of gypsum: In situ FTIR study

P.S.R. Prasad,[1,*] V. Krishna Chaitanya,[2] K. Shiva Prasad,[1] and D. Narayana Rao[2]

[1]National Geophysical Research Institute, Hyderabad 500 007, India
[2]School of Physics, University of Hyderabad, Hyderabad 500 046, India

Abstract

The dehydration mechanism of natural single crystals of gypsum was investigated in the temperature range 300–430 K by in situ infrared (FTIR) spectroscopy. The thermal evolution of the second-order modes of H_2O and SO_4 groups in gypsum, in the wavenumber range 4850–5450 cm^{-1} and 2050–2300 cm^{-1} respectively, were used to probe the dehydration and rehydration sequence. A total disappearance of the combination modes of H_2O and the replacement of four SO_4^{-2} bands (2245, 2200, 2133, and 2117 cm^{-1}) observed at room temperature by three bands (2236, 2163, and 2131 cm^{-1}) observed at 390 K indicates the direct formation of γ-$CaSO_4$ upon heating. Upon cooling water re-enters into the γ-$CaSO_4$ structure at around 363 K to form bassanite. This observation, that the dehydration of gypsum directly yields γ-$CaSO_4$ (anhydrite) without the intermediate formation of hemi-hydrate (bassanite), is further corroborated by the dehydration behavior of bassanite. The second-order SO_4 modes of bassanite observed around 2218, 2136, and 2096 cm^{-1} were replaced with the bands of γ-$CaSO_4$ at about 378 K upon heating.

Introduction

Gypsum ($CaSO_4 \cdot 2H_2O$) is a hydrous mineral that often occurs in extensive masses of great thickness, in association with limestone, shales, and in evaporite deposits (Chang et al. 1996). Despite several studies on this mineral, considerable debate persists on many points, such as the stability and existence of sub-hydrate phases (Follner et al. 2002b), the mechanism of the dehydration and rehydration processes (Chio et al. 2004; Prasad et al. 2001; Chang et al. 1999), and the specific structural and spectral signatures for α- and β-hemihydrate and α- and γ-anhydrite (Follner et al. 2002a; Bartram 1969; Morris 1963). For instance, Strydom and Potgieter (1999) reported significant differences in the amounts of moisture loss as well as their respective surface areas after dehydration for natural and synthetic gypsum, respectively, indicating the need to better understand the mechanism of the dehydration behavior of gypsum. Bassanite ($CaSO_4 \cdot 0.5H_2O$) and soluble anhydrite (γ-$CaSO_4$) are the established low-temperature (below 383 K) dehydration products of gypsum. On the other hand the insoluble anhydrite (α-$CaSO_4$) occurs on heating gypsum above 633 K (Chang et al. 1996), which is an irreversible process. Different phases of calcium sulfate, namely gypsum, bassanite, and anhydrite have been characterized by X-ray diffraction (Lager et al. 1984), inelastic neutron scattering (Pedersen and Semmingsen 1982), infrared (Seidl et al. 1969), and Raman (Krishnamurthy and Soots 1971) spectroscopic methods. In situ IR studies of the phase transition of gypsum by Putnis et al. (1990) showed the existence of the three phases $CaSO_4 \cdot 2H_2O$, $CaSO_4 \cdot 0.5H_2O$, and γ-$CaSO_4$, and also showed that the dehydration process had the following steps:

$$CaSO_4 \cdot 2H_2O \rightarrow CaSO_4 \cdot 0.5H_2O + 1.5\ H_2O$$
$$CaSO_4 \cdot 0.5H_2O \rightarrow CaSO_4 + 0.5\ H_2O$$

A similar mechanism was reported by Chang et al. (1999) from their thermo-Raman spectroscopy studies of synthetic samples. Powdered samples were used in all the previous studies. The critical temperature and pressure above which hemihydrate (bassanite) is stable was estimated as 358 K and 2 kbars (Yamamoto and Kennedy 1969). Thus formation of hemihydrate is thermodynamically unstable. According to Zen (1965) "it appears that bassanite might be stable under high pressures in abnormally cold spots in the crust though the requisite pressure hardly explains the petrographical observations. On the other hand the occurrence of bassanite in industrial and experimental work clearly shows the possibility of its metastable formation under wide ranges of conditions."

While the occurrence of gypsum and anhydrite is common in natural environments, the occurrence of bassanite in nature is very rare (Yamamoto and Kennedy 1969). Tiemann et al. (2002) reports that well-formed hemihydrate single crystals exist in deep-sea statoliths of the coromate medusa "Periphylla periphylla." The environmental conditions for this deep-sea medusa (water at about 6 °C, salt concentration about 35 gl^{-1}) does not favor the formation of hemihydrate and should readily take up water to form gypsum. The formation of hemihydrate was attributed to the nucleating influence of specialized bio-molecules and the isolation of the hemihydrate crystals from water by a thin organic layer preventing the formation of gypsum (Tiemann et al. 2002).

Bassanite has been found in very few places in dry regions, such as arid zone soils in Australia (Akpokodje 1984/85). It has also been found in cavities in leucite, tephrite blocks ejected from Vesuvius, and with gibbsite in fumaroles of this volcano (Chang et al. 1996). If the phase transition sequence of gypsum is a two-step process as shown above, then bassanite should be present as a mineral in gypsum beds which grade into anhydrite at depth. However, the rare occurrence of bassanite in such cases is puzzling (Chang et al. 1996). We have been investigating the dehydration mechanism of natural gypsum using vibrational

* E-mail: psrprasad@ngri.res.in

0003-004X/05/0004–672$05.00/DOI: 10.2138/am.2005.1742

spectroscopic methods (Sarma et al. 1998; Prasad 1999; Prasad et al. 2001). In all of these studies we used single-crystal samples for the Raman spectroscopic analysis and showed evidence for phase transformations of gypsum to γ-$CaSO_4$ and then to bassanite by observing the characteristic $\nu_1(SO_4)$ Raman modes at Δ 1008 (gypsum), Δ 1026 (anhydrite), and Δ 1014 cm^{-1} (bassanite). The bassanite phase is predominantly formed during the cooling cycle (Prasad et al. 2001). Similar observations have been reported by Chio et al. (2004) for their Raman investigations. Our observations that bassanite is formed upon cooling and rehydration of γ-$CaSO_4$ differs from the observations of Chang et al. (1999) and Putnis et al. (1990), who reported a sequential phase transformation, i.e., from gypsum to bassanite and then to anhydrite upon heating.

The main objective of our studies is to understand the dehydration and rehydration mechanism during the phase transition sequence using single crystals by in situ FTIR spectroscopy. Recently Badens et al. (1998) reported one dehydration step for gypsum to γ-$CaSO_4$ when the water vapor pressure is between 1 and 500 Pa. However, two-step dehydration was reported at water vapor pressure of 900 Pa (Badens et al. 1998). In this paper we present the thermally induced variation for the combinational modes of water and sulfate groups of gypsum single crystals using in situ FTIR spectroscopy over the wavenumber ranges 4850–5450 and 2050–2300 cm^{-1}, respectively. We have particularly chosen the second-order modes because their activity strongly depends on the factor group variations. Second, experiments can be carried out directly on the thin single crystals, without matrix materials such as KBr, avoiding the interactions due to surface or adsorbed water, which is particularly significant while probing structural changes involving liberation of water molecules.

Materials and methods

Sample preparation

Small crystals were cut along the plane of cleavage from a large transparent rectangular sheet of gypsum obtained from M/s Hindustan Minerals and Natural History Supply Co., Calcutta, India. These samples were polished to reduce the thickness. The thickness of the samples was measured by a screw-gauge with a precision of 10 μm. Originally, samples with various thicknesses (500 and 200 μm) were used for investigations and it was observed that they are opaque for IR radiation at higher temperatures, just above dehydration, making it difficult to record spectral features in the γ-$CaSO_4$ phase. Thus, a sample thickness of about 100 μm was optimal for recording the FTIR spectra in the temperature range of 300–430 K and the results presented here were obtained with 100 μm thick samples.

Small portions of the sample from a large crystal of gypsum were used for initial X-ray diffraction (XRD) and IR absorption study using the conventional KBr pellet technique. A plate 5 × 5 × 0.1 mm^3 in size was used in the thermal transformation study. The residue was allowed to cool for more than 24 hours before further analysis. A small portion of the sample was used to make a KBr pellet for characterization in the IR range 400–4000 cm^{-1}, and the remaining powder was used for XRD analysis.

X-ray diffraction

The X-ray diffraction (XRD) patterns were obtained using a Philips PW-1830 powder diffractometer with Ni filter. The radiation used was Cu$K\alpha$ and the 2θ scan was from 10°–80°. These data confirmed the mineralogical assignments of the sample.

Infrared spectroscopy

FTIR studies were carried out with a NEXUS FTIR spectrometer from Thermo-Nicolet, using a thermo-electrically cooled deuterated triglycene sulfate (DTGS) detector, extended range KBr (XT-KBr) beam splitter, and a dual source, capable of working in the wavenumber range 375–12,500 cm^{-1}. We did not carry out polarization-dependent studies as we lack such capability. The sample was placed in a specially fabricated environmental chamber. This chamber can be used to increase the temperature of the sample under study up to about 950 K with an accuracy of ± 2°. Circulating tap water is used to cool the outer jacket of the chamber, which consists of infrared transparent windows. The spectra were recorded in the wavenumber region 1500 to 8000 cm^{-1} using a white light source (tungsten halogen) and each spectrum is an average of 256 scans with 1 cm^{-1} resolution. The second-order modes look rather noisy, particularly those of SO_4 groups as they occur toward the leading edge of the light source. In principle one can decrease the noise by recording the spectrum at the usual spectral resolution of 4 cm^{-1}. The conventional KBr pellet method was also used to characterize the starting sample, i.e., ground-up gypsum and the residue, i.e., after heat treatment, in the wavenumber range 400 to 4000 cm^{-1}, using a NEXUS Ever-Glo source.

Results

Characterization

The XRD pattern of the natural gypsum sample showed prominent peaks with *d*-spacings at 7.55, 4.26, 3.79, and 3.06 Å which are comparable with corresponding *d*-values of 7.52, 4.25, 3.76, and 3.05 Å reported by Follner et al. (2002a). Similarly, the residue generated during the experiments also showed XRD peaks with *d*-values around 5.99, 3.47, 3.00, and 2.8 Å, which are comparable to the corresponding *d*-values 6.00, 3.50, 3.01, and 2.89 Å for bassanite as reported by Follner et al. (2002b).

Furthermore, the starting material (gypsum), the residue (bassanite), and $CaSO_4$ (anhydrite) were characterized by the conventional KBr pellet technique. The spectrum in the wavenumber range 400–1800 cm^{-1} is shown in Figure 1 and the characteristic hydroxyl-stretching modes are shown as an inset. The peak positions of gypsum, bassanite, and anhydrite are listed and compared in Table 1a. These values are in good agreement with those reported in the literature (Bensted and Prakash 1968; Putnis et al. 1990). The $\nu_1(SO_4)$ mode at 1005, 1008, and 1014 cm^{-1} is seen in gypsum, bassanite, and anhydrite respectively (see Table 1a). The $\nu_4(SO_4)$ mode shows two components at 602 and 669 cm^{-1} for gypsum, whereas they occur at 601 and 660 cm^{-1} for bassanite. However, there is a splitting in the $\nu_4(SO_4)$ mode resulting in three modes at 676, 615, and 595 cm^{-1} in anhydrite. This behavior is very similar to that reported by Putnis et al. (1990). Observed spectra in the $\nu_3(SO_4)$ mode region (1100–1200 cm^{-1}) are comparable with those of Bensted and Prakash (1968). Gypsum has two IR-active modes in the bending modes of water (ν_2) observed at 1621 and 1685 cm^{-1}, whereas bassanite has only one mode at 1620 cm^{-1}. The other two stretching modes (ν_3 and ν_1) of water groups are found at 3547 and 3405 cm^{-1} for gypsum, and the corresponding modes for bassanite are at 3610 and 3550 cm^{-1} (see inset of Fig. 1).

Observed infrared spectra in the overtone region due to H_2O are shown in Figure 2a. It is noteworthy that the spectral behavior in the 6000–7000 cm^{-1} wavenumber range, where the first overtones of the hydroxyl stretching modes are expected, is very similar to the fundamental modes. From the group theoretical point of view the allowed combination modes in the infrared are those which are individually active in infrared and Raman (see discussion). The modes at 6919, 6710, and 6512 cm^{-1} for gypsum could be assigned to $[\nu_3(A_g) \times \nu_3(A_u)]$, $[\nu_3(B_g) \times \nu_3(B_u)]$, and $[\nu_1(A_g) \times \nu_1(A_u)]$ respectively. The overtones of the hydroxyl stretching modes in bassanite are observed at 7027 and 6766

TABLE 1A. Observed infrared fundamental modes (in cm^{-1}) of gypsum, bassanite, and anhydrite recorded at ambient conditions

Present study			*			Assignment
gypsum	bassanite	anhydrite	gypsum	bassanite	anhydrite	
602	601	595,615	602†	600†	594†,616†	ν_4, SO_4
669	660	676	667,668†	660,658†	665,668†	ν_4, SO_4
1005	1008	1014	1004	1008	1008	ν_1, SO_4
–	1096	–	–	1094	–	ν_3, SO_4
1117	1116	1124	1120	1115	1115	ν_3, SO_4
1145	1153		1145	1155	1135	ν_3, SO_4
1167	1168	1157	1155	1168	1155	ν_3, SO_4
1621	1620	–	1623	1623	–	ν_2, H_2O
1685	–	–	1688	–	–	ν_2, H_2O
3405	3550	–	3410	–	–	ν_1, H_2O
3495	–	–	3500	3560	–	ν_1, H_2O
3547	3610	–	3555	3615	–	ν_3, H_2O

* Band positions from Bensted and Prakash (1968).
† Band positions from Putnis et al. (1990).

TABLE 1B. Observed band positions of H_2O groups (in cm^{-1}) of gypsum

	A_g	B_g	A_u	B_u
ν_1	3401*	3400†	3405	3392†
ν_2	1630†	1679†	1685	1621
ν_3	3489*	3500†	3547	3490†

* Band positions from Prasad et al. (2001).
† Band positions from Krishnamurthy and Soots (1971).

cm^{-1}. The infrared modes due to combinations of stretching (ν_3 and/or ν_1) and bending modes (ν_2) of water in gypsum are observed at 5123 and 5070 cm^{-1}. There are two more shoulders at 5034 and 5170 cm^{-1}. The corresponding mode in bassanite is observed at 5207 cm^{-1}. The sulfate group overtone spectra around 2000–2300 cm^{-1} are shown in Figure 2b. The spectral behavior in this region is different in the three phases. The top trace in Figure 2b, corresponding to gypsum recorded at ambient temperature (300 K), shows four peaks at 2245, 2200, 2133, and 2117 cm^{-1}. These modes are due to combinations of the ν_1 and ν_3 modes of sulfate (Bensted and Prakash 1968). The Raman-active modes for gypsum are ν_1 at Δ 1008 cm^{-1} (A_g) and ν_3 at Δ 1141 cm^{-1} (A_g), Δ 1116 cm^{-1} and Δ 1132 cm^{-1} (B_g) (Prasad et al. 2001; Krishnamurthy and Soots 1971). Similarly, the infrared-active modes are at 1005 cm^{-1} (ν_1-A_u), 1145 cm^{-1} (ν_3-A_u), and 1117 and 1167 cm^{-1} (ν_3-B_u). A total of six combination modes involving ($\nu_1 + \nu_3$) are expected in the wavenumber range 2050–2300 cm^{-1}, four of which are seen in our results. Bensted and Prakash (1968) reported similar observations. At higher temperatures (390 K) these four bands are replaced by bands at 2236 and 2131 cm^{-1} with a shoulder around 2163 cm^{-1} (see trace C in Fig. 2b recorded at 398 K). These spectral features resemble those associated with anhydrite from the Nicolet spectrum library with peak positions at 2234 and 2142 cm^{-1}. Bensted and Prakash (1968) also reported peaks at 2130, 2150, and 2230 cm^{-1} for the anhydrite phase. The observed peak positions for second-order sulfate modes in bassanite are at 2218, 2136, and 2096 cm^{-1} (see trace B in Fig. 2b). These are comparable to the peak positions, for cement additive, at 2213 and 2136 with a shoulder around 2101 cm^{-1} from the Nicolet library. Bensted and Prakash (1968) reported similar band positions for hemihydrate at 2220, 2130, 2090, and 2030 cm^{-1}. Thus, in addition to water modes, we can also use these second-order spectral signatures of SO_4 groups to probe the dehydration dynamics.

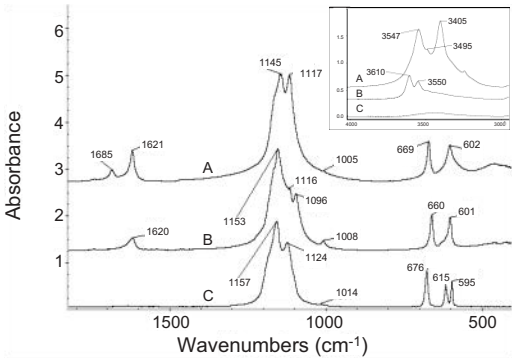

FIGURE 1. Infrared spectrum of gypsum (A), bassanite (B) and γ-$CaSO_4$ (C) in the wavenumber region 400–1800 cm^{-1}. OH stretching modes are shown in the inset.

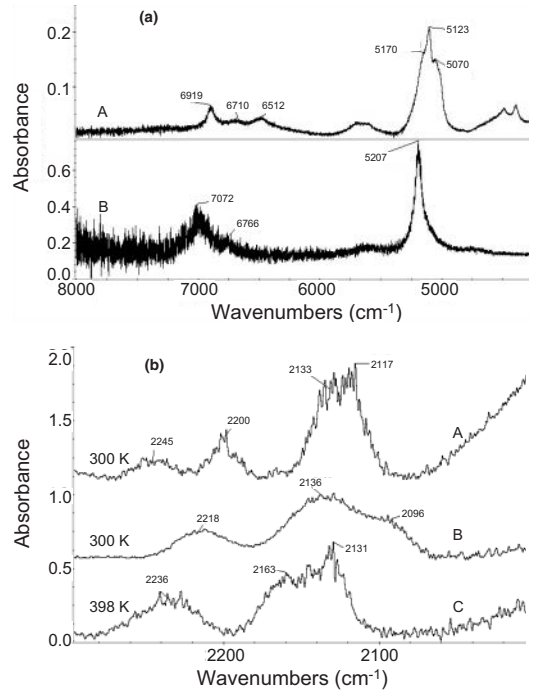

FIGURE 2. (**a**) Observed second-order modes of gypsum (A) and bassanite (B) in the wavenumber region 4000–8000 cm^{-1}. (**b**) Characteristic second-order modes of SO_4 groups in gypsum (A), bassanite (B), and γ-$CaSO_4$ (C).

In situ Fourier transform infrared studies

We have investigated phase transitions in gypsum with an aim to understanding the dehydration mechanism. The thermal evolution of the combination modes of water in the wavenumber region 4850–5450 cm^{-1} and the second-order modes of sulfate groups in the wavenumber region 2050–2350 cm^{-1} were closely monitored in the temperature range 300–430 K. The thermal evolution of these bands was observed at intervals of 5 K close to the transition temperatures. However, for clarity we only show 3–4 traces recorded at different temperatures in Figures 3–5. The rate of heating was slower than 2° per minute in the temperature

range 353–398 K. We had chosen to investigate the phase transition sequence using single crystals because of differences in the mechanism of dehydration. As previously stated, the results of Putnis et al. (1990) and Chang et al. (1999) show stepwise dehydration in powdered samples, whereas studies from our laboratory (Sarma et al. 1998; Prasad 1999; Prasad et al. 2001) and by Badens et al. (1998) show single-step dehydration for crystalline gypsum. The total experiment was carried-out in three steps; step 1, dehydration of gypsum in the temperature range 300–430 K; step 2, rehydration of γ-$CaSO_4$; and step 3, dehydration of bassanite up to 430 K. Observed spectral variations at some selective temperatures are shown in Figures 3–5. Recorded profiles in these figures are shown by dots and the continuous lines represent deconvolved profiles. During the dehydration of gypsum (step 1) the water combination modes showed marginal spectral variation until about 388 K and completely disappeared around 390 K (Fig. 3). However, on cooling a single band appeared at 5206 cm^{-1}, indicating the bassanite phase (Fig. 4). This band is very narrow compared to the complex H_2O bands of gypsum. The second-order modes of sulfate group also showed interesting temperature-induced variations. The four gypsum peaks at 2245, 2200, 2133, and 2117 cm^{-1} were replaced with three bands at 2236, 2163, and 2131 cm^{-1} at around 390 K during the first stage of our experiment, characteristic of anhydrite (see part B of Fig. 3).

In step 2, the dehydrated gypsum, i.e., anhydrite, was cooled slowly to room temperature and the rehydration behavior was observed. As can be seen from Figure 4, water molecules reentered the structure at around 363 K. The characteristic second-order modes of sulfate groups of bassanite were observed at 2218, 2136, and 2096 cm^{-1} and that of the water combination around 5206 cm^{-1}. These spectral features are seen more clearly at ambient temperature. We observed a large variation in absorbance of fundamental water modes, also indicating the re-entry of water molecules. On cooling we failed to recover the spectral features characteristic of gypsum. In fact, the spectra showed the signatures of bassanite, which is in general agreement with our previous results (Prasad et al. 2001). The bassanite formed in step 2 was taken as the starting sample for step 3 (Fig. 5).

The combination mode at 5206 cm^{-1} collapsed at around 383 K and this behavior appeared from 378 K. The second-order modes of sulfate also showed typical variations characteristic of anhydrite as previously described, namely the replacement of bassanite features (2218, 2136, and 2096 cm^{-1}) with anhydrite bands (2236, 2163, and 2131 cm^{-1}) (see Fig. 5). These results indicate the dehydration of bassanite to γ-$CaSO_4$, beginning at about 378 K. The band

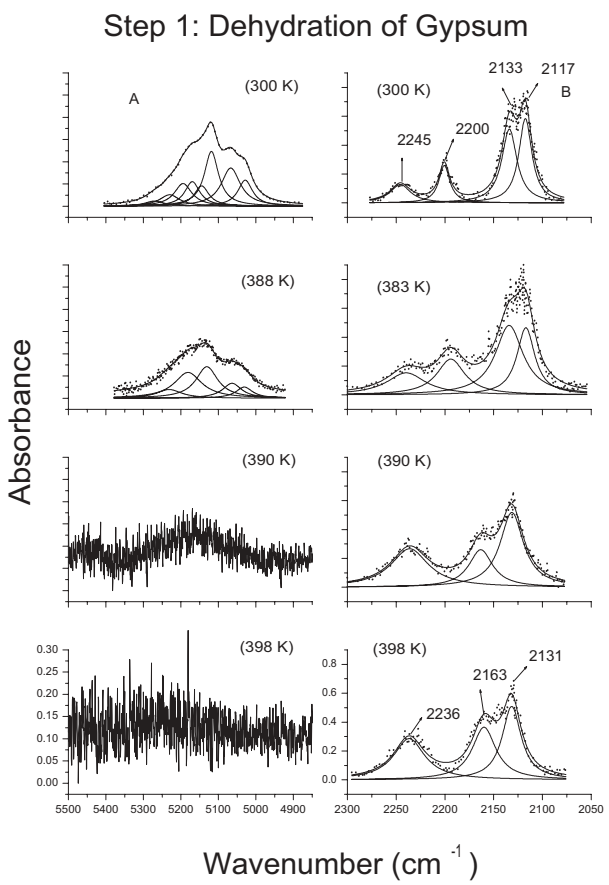

FIGURE 3. Deconvolved bands of the combination modes of H_2O (A) and SO_4 (B) of gypsum at different temperatures as indicated along with traces. Observed profiles are shown by dots. Continuous lines show fitted and deconvolved profiles.

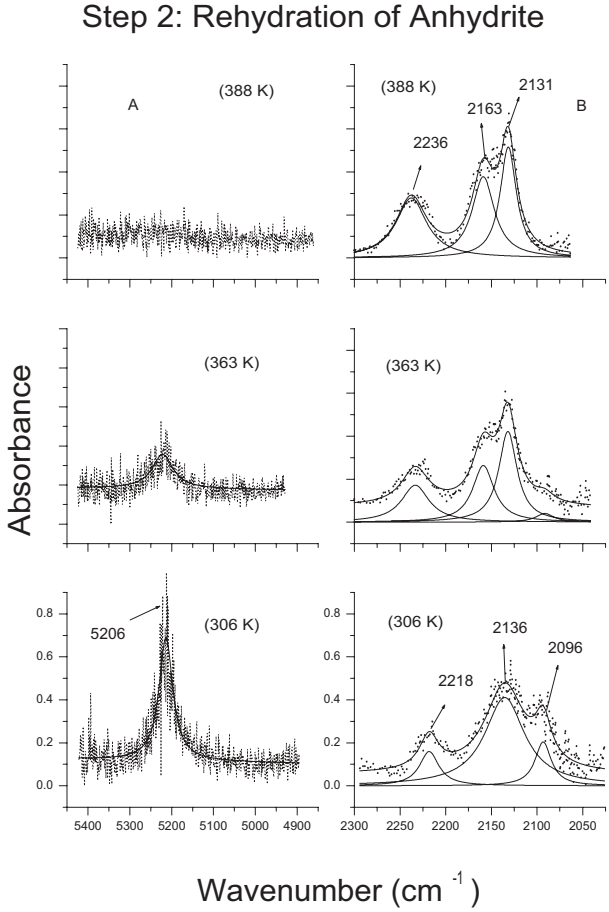

FIGURE 4. Deconvolved bands of the combination modes of H_2O (A) and SO_4 (B) for γ-$CaSO_4$ upon cooling. All other details are same as those in Figure 3.

at 5206 cm^{-1} reappeared upon cooling along with that of the SO_4 mode structure around 2218, 2136, and 2096 cm^{-1}, signifying the rehydration of γ-$CaSO_4$ to form bassanite. This observation confirms that of 2. However, we failed to observe formation of gypsum from this bassanite even after preserving the sample for over three months under laboratory conditions.

Discussion

A large number of Raman and infrared spectroscopic studies on gypsum were aimed at probing the hydrogen-bonding scheme. Generally, the variations of water modes are weakly dependent on pressure (Couty et al. 1983). However, more recent studies of pressure-dependent FTIR and Raman spectroscopy of gypsum by Knittle et al. (2001) report a new phase above 5–6 GPa. Interestingly these variations are similar to those reported for bassanite (Putnis et al. 1990). On the other hand, the hydroxyl modes and hydrogen-bonding scheme is usually dependent on temperature (Chang et al. 1996). In the hemi-hydrate phase stretching modes of hydroxyls are shifted to higher wavenumber by about 100 cm^{-1} compared to gypsum, indicating weakening of the hydrogen bonding (see inset in Fig. 1).

The symmetric (ν_1) and asymmetric (ν_3) stretching modes of water in gypsum show a large gap, which is rather unusual (Fig. 1). There are two different interpretations for this observation.

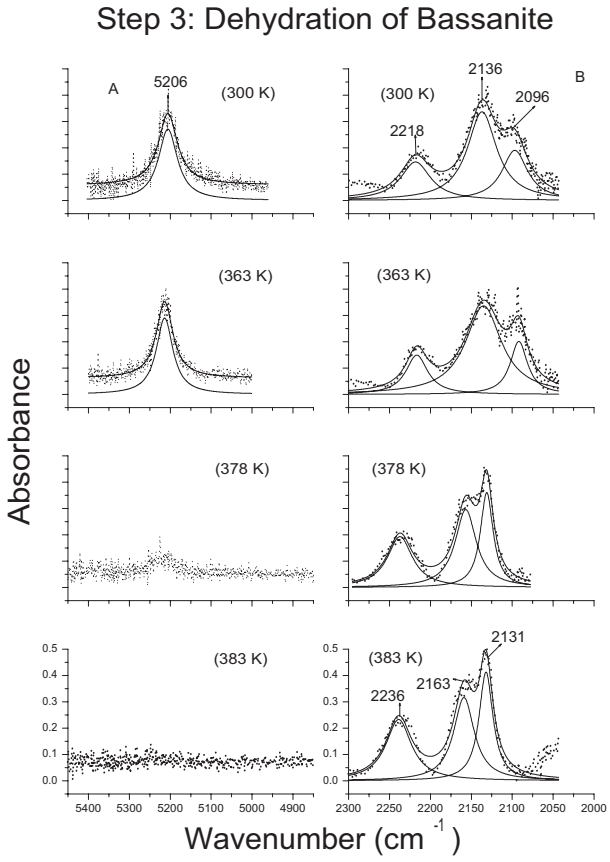

Figure 5. Deconvolved band profiles of second-order infrared active modes of H_2O (A) and SO_4 (B) groups in bassanite upon heating. All other details are same as those in Figure 3.

One attributes the two modes to ν(O-H) having two non-equivalent O-H···O bond lengths of 2.816 and 2.896 Å (Couty et al. 1983; Chio et al. 2004). Another interpretation is factor-group splitting (Krishnamurthy and Soots 1971; Iishi 1979). Kling and Schiffer (1969, 1971) suggested a similarity between liquid water and the water in gypsum. Furthermore, they also proposed that the water molecules in gypsum are vibrationally distorted. The Fermi resonance may also contribute to a greater separation between the ν_1 and ν_3 modes (Kling and Schiffer 1971).

Gypsum is an ionic crystal belonging to the monoclinic space group C_{2h}^6, with two formula units per unit cell, i.e., there are a total of 24 atoms in the unit cell. Since the unit cell of gypsum possesses a centre of inversion, the principle of mutual exclusion applies so that only the gerade modes are Raman active while ungerade modes are infrared active. A detailed factor group analysis results in activity of nine internal modes of SO_4 groups as $5A_u + 4B_u$ and six internal modes of H_2O as $3A_u + 3B_u$. The site groups for these ions are C_2 and C_1 respectively. All the splittings in the internal modes have been clearly observed and reported in earlier studies (Krishnamurthy and Soots 1971; Bensted and Prakash 1968; Berenblut et al. 1971). Considering the activity of the second-order modes, all the overtones belonging to $(A_g \times A_g)$, $(B_g \times B_g)$, $(A_u \times A_u)$, or $(B_u \times B_u)$ are Raman active. However, the combination bands are IR active; e.g., $(A_g \times A_u)$ and $(B_g \times B_u)$ results in A_u species while $(A_g \times B_u)$ and $(A_u \times B_g)$ results in B_u. As can be seen from Figure 2a the water combination mode region in gypsum is highly complex with two bands around 5123 and 5070 cm^{-1} and two prominent shoulders at 5034 and 5170 cm^{-1}. However, the observed band positions of the second-order water modes of gypsum are vastly different from those for liquid water. In liquid water the IR combinations bands are at 5193 cm^{-1} and the overtones are at 6885 cm^{-1}. Table 1b lists the infrared- and Raman-active fundamentals of water modes in gypsum for all A_g, B_g, A_u, and B_u species. Several combination modes, i.e., ν_1 or $\nu_3 + \nu_2$, are thus group-theoretically allowed for the water modes. From the observed spectral profile in the wavenumber region 4850–5450 cm^{-1}, Lorentzian profiles were fitted using GRAMS software. Figure 3 shows the deconvolved plots of second-order modes of water (A) and sulfate (B) at four different temperatures, i.e., 300, 388, 390, and 398 K. Even though we show the results at some selected temperatures in Figures 3–5, we actually monitored the dehydration behavior over very small temperature intervals near the phase transition temperatures. The best spectral fit for the data at 300 K was obtained with eight Lorentzian peaks with $R^2 = 0.99$. However, the fit was not good for lesser number of profiles. R^2 for the data at 388 K was 0.97 with eight peaks.

As seen in Figure 3, the water modes show marginal variations up to about 388 K and completely disappear around 390 K, and no water modes were observed up to about 430 K. A question often asked is whether or not the dehydration of gypsum to bassanite is through an intermittent γ-$CaSO_4$. Our earlier Raman spectroscopic studies (Prasad et al. 2001) and those of Chio et al. (2004) support the former, whereas Chang et al. (1999) supports the latter interpretation. In our previous Raman studies we observed that the $\nu_1(SO_4)$ mode of gypsum Δ 1008 cm^{-1} was replaced with a mode around Δ 1026 cm^{-1} at higher temperature (370 K). On cooling we observed a mode around Δ 1014 cm^{-1}.

These three modes we attributed to gypsum, γ-$CaSO_4$, and bassanite, respectively. Chio et al. (2004) also reported Raman shifts for the $\nu_1(SO_4)$ mode in gypsum, γ-$CaSO_4$, and bassanite of Δ 1007, Δ 1026, and Δ 1014 cm^{-1}. They further suggested that the changes in Raman shifts for this mode with respect to varying hydration state, in addition to the strong intensity and the narrow peak width, could be utilized to distinguish various hydrate forms of $CaSO_4$. The results of Chang et al. (1999) are different. These authors reported that the $\nu_1(SO_4)$ Raman mode of gypsum is at 1010 cm^{-1} and shows spectral variations to above 391 K; a band around Δ 1017 cm^{-1} (assigned to bassanite) appears and grows to maximum around 405 K and decreases and vanished around 413 K. Another weaker mode around Δ 1024 cm^{-1} (assigned to anhydrite), appears around 391 K, grows and reaches a maximum at around 413 K. Putnis et al. (1990) in their FTIR studies also reported that the spectral signatures of bassanite develop (replacing those of gypsum) with increasing temperature, indicating a sequential transition. These authors also reported a temperature region where gypsum-bassanite-anhydrite coexists. Chang et al. (1999) reported that the dehydration temperature of bassanite is lower than that of gypsum. From Figures 3 and 5 we also notice that the dehydration temperature of bassanite is about 12° lower than that of gypsum and is 378 and 390 K, respectively. Even though we probed the transitions with temperature intervals of about 2–5° we failed to observe co-existence of spectral signatures typical of gypsum and bassanite. The disappearance of IR modes due to water molecules of gypsum provides strong evidence for its dehydration to γ-$CaSO_4$. Further support of this observation is through the thermal evolution of the second-order SO_4 modes, as shown in Figure 3B. The four-mode structure observed at 300 K with deconvolved peak positions at 2245, 2200, 2133, and 2117 cm^{-1} is clearly replaced with three bands around 2236, 2163, and 2131 cm^{-1} at 390 K. As previously discussed, the former is characteristic of gypsum, whereas the latter is characteristic of γ-$CaSO_4$.

From Figure 4 it is clear that rehydration of γ-$CaSO_4$ occurred around 363 K, as can be seen from the reappearance of the water combination mode around 5206 cm^{-1} and a shoulder mode around 2096 cm^{-1}. The absorbance for fundamental modes also showed a sudden increase indicating the re-entry of water molecules into the structure. These spectral features increase and become very clear at lower temperatures indicating the growth of bassanite. The experiments in this study (Figs. 3 and 4) support our earlier studies (Prasad et al. 2001) where we proposed that the water molecules of gypsum dehydrate completely and the water molecules re-enter into soluble anhydrite to form bassanite. As described we have not seen recovery of the gypsum features, indicating that the gypsum dehydration is an irreversible process.

In the final step we studied the dehydration behavior of bassanite. In Figure 5, we demonstrate deconvolved plots at some selected temperatures where maximum spectral variations occurred. The spectral features of the second-order SO_4 group observed at 2218, 2136, and 2096 cm^{-1} at 300 K are typical of bassanite (Bensted and Prakash 1968). A noticeable spectral difference between bassanite and $CaSO_4$ is the presence of a mode around 2096 cm^{-1}. As the temperature is increased to about 378 K, the combination mode due to H_2O observed around 5206 cm^{-1} became weaker and at about 383 K it completely disappeared, indicating dehydration of bassanite to γ-$CaSO_4$. This behavior has even been observed from the thermal evolution of SO_4 second-order modes, where the peaks shifted to 2237, 2157, and 2131 cm^{-1} at around 383 K. This behavior continued up to about 430 K. Furthermore, similarities in the second-order SO_4 mode structure at 390 K during the gypsum dehydration process (as shown in Fig. 3b) and that at 383 K during the bassanite dehydration process (shown in Fig. 5b) confirm the formation of intermittent γ-$CaSO_4$ during the dehydration of gypsum.

ACKNOWLEDGMENTS

The authors sincerely thank V.P. Dimri, Director, National Geophysical Research Institute, Hyderabad, for his encouragement, keen interest in this program, and for permission to publish this work. Helpful discussions with N.K. Thakur are greatly acknowledged. The authors also acknowledge many stimulating comments and suggestions from B. Wopenka, Associate Editor, M.D. Lane, and two anonymous reviewers that helped to improve this paper.

REFERENCES CITED

Akpokodje, E.G. (1984/1985) The occurrence of bassanite in some Australian arid zone soils. Chemical Geology, 47, 361–364.

Badens, E., Llewellyn, P., Fulconis, J.M., Jourdan, C., Veesler, S., Boistelle, R., and Rouquerol, F. (1998) Study of gypsum dehydration by controlled transformation rate thermal analysis (CRTA). Journal of Solid State Chemistry, 139, 37–44.

Bartram, D.A. (1969) Infrared absorption spectra of α and β-calcium sulphate hemihydrates. Nature, 223, 494.

Bensted, J. and Prakash, S. (1968) Investigation of calcium sulphate water system by infrared spectroscopy. Nature, 219, 60–61.

Berenblut, B.J., Dawson, P., and Wilkinson, G.R. (1971) The Raman spectrum of gypsum. Spectrochimica Acta, 27A, 1849–1863.

Chang, L.L.Y., Howie, R.A., and Zussman, J. (1996) Non-silicates: Sulphates, Carbonates, Phosphates and Halides. Rock-Forming Minerals, 5B, 40–73.

Chang, H., Huang, P.J., and Hou, S.C. (1999) Application of thermo-Raman spectroscopy to study dehydration of $CaSO_4 \cdot 2H_2O$ and $CaSO_4 \cdot 0.5H_2O$. Materials Chemistry and Physics, 58, 12–19.

Chio, C.H., Sharma, S.K., and Muenow, D.W. (2004) Micro-Raman studies of gypsum in the temperature range between 9 K and 373 K. American Mineralogist, 89, 390–395.

Couty, R., Velde, B., and Besson, J.M. (1983) Raman spectra of gypsum under pressure. Physics and Chemistry of Minerals, 10, 89–93.

Follner, S., Wolter, A., Helming, K., Silber, C., Bartels, H., and Follner, H. (2002a) On the real structure of gypsum crystals. Crystal Research Technology, 37, 207–218.

Follner, S., Wolter, A., Preusser, A., Indris, S., Silber, C., and Follner, H. (2002b), The setting behaviour of α- and β-$CaSO_4 \cdot 0.5\ H_2O$ as a function of crystal structure and morphology. Crystal Research Technology, 37, 1075–1087.

Iishi, K. (1979) Phonon spectroscopy and lattice dynamical calculations of anhydrite and gypsum. Physics and Chemistry of Minerals, 4, 341–359.

Kling, R. and Schiffer, J. (1969) The potential environment about the water molecule in gypsum. Chemical Physics Letters, 3, 64–66.

——— (1971) Intra- and intermolecular interactions in and between water molecules in calcium sulfate dihydrate. Journal of Chemical Physics, 54, 5331–5338.

Knittle, E., Phillips, W., and Williams, Q. (2001) An infrared and Raman spectroscopic study of gypsum at high pressures. Physics and Chemistry of Minerals, 28, 630–640.

Krishnamurthy, N. and Soots, V. (1971) Raman spectrum of gypsum. Canadian Journal of Physics, 49, 885–896.

Lager, G.A., Armbruster, Th., Rotella, F.J., Jorgensen, J.D., and Hinks, D.G. (1984) A crystallographic study of low temperature dehydration products of gypsum, $CaSO_4 \cdot 2H_2O$, hemihydrate $CaSO_4 \cdot 0.5H_2O$ and γ-$CaSO_4$. American Mineralogist, 69, 910–918.

Morris, R.J. (1963) X-ray diffraction identification of the alpha and beta-forms of calcium sulphate hemihydrate. Nature, 198, 1298–1299.

Pedersen, B.F. and Semmingsen, D. (1982) Neutron diffraction refinement of the structure of gypsum, $CaSO_4 \cdot 2H_2O$. Acta of Crystallographica, 38B, 1074–1077.

Prasad, P.S.R. (1999) Raman intensities near gypsum-bassanite phase transition in natural gypsum. Journal of Raman Spectroscopy, 30, 693–696.

Prasad, P.S.R., Pradhan, A., and Gowd, T.N. (2001) In situ micro-Raman investigation of dehydration mechanism in natural gypsum. Current Science, 80, 1203–1207.

Putnis, A., Winkler, B., and Fernandez-Diaz, L. (1990) In situ IR spectroscopic

and thermogravimetric study of the dehydration of gypsum. Mineralogical Magazine, 54, 123–128.

Sarma, L.P., Prasad, P.S.R., and Ravikumar, N. (1998) Raman spectroscopic study of phase transition in natural gypsum. Journal of Raman Spectroscopy, 29, 851–856.

Seidl, V., Knop, O., and Falk, M. (1969) Infrared studies of water in crystalline hydrates: gypsum $CaSO_4 \cdot 2H_2O$. Canadian Journal of Chemistry, 47, 1361–1368.

Strydom, C.A. and Potgieter, J.H. (1999) Dehydration behaviour of natural gypsum and a phosphogypsum during milling. Thermochimica Acta, 332, 89–96.

Tiemann, H., Sotje, I., Jarms, G., Paulmann, C., Epple, M., and Hasse, B. (2002) Calcium sulphate hemihydrate in statoliths of deep-sea medusae. Journal of the Chemical Society: Dalton Transactions, 1266–1268.

Yamamoto, H. and Kennedy, G.C. (1969) Stability relations in the system $CaSO_4$-H_2O at high temperatures and pressures. American Journal of Science, 267-A, 550–557.

Zen, E-An. (1965) Solubility measurements in the system $CaSO_4$-NaCl-H_2O at 35 °C, 50 °C, 70 °C and one atmosphere pressure. Journal of Petrology, 6, 124–164.

MANUSCRIPT RECEIVED JUNE 7, 2004
MANUSCRIPT ACCEPTED OCTOBER 19, 2004
MANUSCRIPT HANDLED BY BRIGITTE WOPENKA